

A neutral Re(I) complex platform for live intracellular imaging

Todd A. Gillam,[a,d] Chiara Caporale,[b] Robert D. Brooks,[a] Christie A. Bader,[a]

Alexandra Sorvina,[a] Melissa V. Werrett, [c] Phillip J. Wright,[b] Janna L. Morrison,[a]

Massimiliano Massi,[b] Doug A. Brooks,[a] Stefano Zacchini,[e] Shane M. Hickey,[a]

Stefano Stagni,[e] and Sally E. Plush[a,d]**

a UniSA Clinical and Health Sciences, University of South Australia, North Tce,

Adelaide, SA 5000, Australia.

b Department of Chemistry, Curtin University, Kent St., Bentley, WA 6102, Australia.

c School of Chemistry, Monash University, Clayton, Melbourne, Victoria 3800, Australia.

d UniSA STEM, Future Industries Institute, University of South Australia, Mawson

Lakes, SA 5095, Australia.

e Department of Industrial Chemistry “TosoMontanari”, University of Bologna, Viale
Risorgimento, 4, Bologna 40136, Italy.

*equal corresponding authors

Email: sally.plush@unisa.edu.au, Stefano.stagni@unibo.it

CONTENTS

- Synthesis and characterization of 5-(4-iodophenyl)-1H-tetrazole p 3
- Synthesis and characterization of *fac*-[Re(phen)(CO)₃(Br)] p 3
- Crystallographic Data (**Tables S1 and S2**) p 3
- ¹H and ¹³C NMR spectra for carbohydrate appended Re(I) complexes (**Figure S1–S8**) p 6
- HRMS spectra for carbohydrate appended Re(I) complexes (**Figure S9–S12**) p 14
- HPLC traces (**Figure S13**) p 17
- Photophysics (**Figure S14–15**) p 18
- Fluorescence microscopy images (**Figure S16-19**) p 20
- Cell viability (**Figure S19**) p 24

Synthesis and characterization of 5-(4-iodophenyl)-1*H*-tetrazole

5-(4-iodophenyl)-1*H*-tetrazole (1) was prepared following a reported procedure,²⁴ (0.580 g, 98%), m.p. 268–269 °C (slow decomposition) (lit. 269–271 °C (slow decomposition)).⁴² ¹H NMR (400 MHz, DMSO-*d*₆) δ 7.98 (2H, d, *J* = 8.4 Hz, CN₄-C₆H₄-I H_{meta}), 7.82 (2H, d, *J* = 8.8 Hz, CN₄-C₆H₄-I H_{ortho}); ¹³C NMR (400 MHz, DMSO-*d*₆) δ 155.4 (CN₄-C₆H₄-I), 138.4, 128.9, 124.1, 98.5.

Synthesis and characterization of *fac*-[Re(phen)(CO)₃(Br)]

fac-[Re(phen)(CO)₃(Br)] (2) was prepared following a reported procedure,²⁵⁻²⁶ (598 mg, 92%). m.p. 336 °C (slow decomposition). ν_{max} (ATR)/cm⁻¹: 3084 w, 2015 s (CO, A'(1)), 1925 s (CO, A'(2)), 1882 (1863 sh) s (CO, A''), 1629 w, 1584 w, 1517 w, 1424 m, 1407 w, 1342 w, 1314 w, 1300 w, 1259 w, 1210 w, 1142 w, 1096 w, 957 w, 850 m, 782 w, 722 w.

Crystallographic data

Table S1. Selected bond lengths (Å) and angles (°) for **ReAlkyne** and complex **ReBn**.

Selected bond	ReAlkyneÅ(°)	ReBnÅ(°)
Re(1)-C(1)	1.86(2)	1.865(9)
Re(1)-C(2)	1.90(2)	1.921(7)
Re(1)-C(3)	1.81(3)	1.905(7)
Re(1)-N(2)	2.167(16)	2.180(4)
Re(1)-N(5)	2.207(16)	2.171(4)
Re(1)-N(6)	2.166(14)	2.178(5)

C(1)-O(1)	1.18(2)	1.194(9)
C(2)-O(2)	1.17(2)	1.141(8)
C(3)-O(3)	1.22(2)	1.159(7)
N(1)-N(2)	1.304(17)	1.348(5)
N(2)-N(3)	1.35(2)	1.314(6)
N(3)-N(4)	1.32(2)	1.327(6)
N(1)-C(11)	1.35(2)	1.331(6)
N(4)-C(11)	1.30(2)	1.338(6)
C(11)-C(12)	1.46(2)	1.470(7)
C(15)-C(18)	1.39(3)	1.479(7)
C(18)-C(19)	1.17(3)	1.380(7)
C(18)-N(7)	-	1.346(7)
N(7)-N(8)	-	1.325(6)
N(8)-N(9)	-	1.345(7)
N(9)-C(19)	-	1.343(7)
Re(1)-C(1)-O(1)	175(2)	176.8(6)
Re(1)-C(2)-O(2)	177(2)	177.8(6)
Re(1)-C(3)-O(3)	177(2)	176.9(5)
C(1)-Re(1)-N(6)	173.5(8)	172.7(2)
C(2)-Re(1)-N(5)	173.2(7)	172.8(2)
C(3)-Re(1)-N(2)	177.9(8)	176.4(2)
N(5)-Re(1)-N(6)	75.8(6)	75.90(17)
C(15)-C(18)-C(19)	173(3)	128.0(5)
Sum angles at N ₄ C	540(3)	540.0(9)
Sum angles at N ₃ C ₂	-	540.0(9)
Angle between the N ₄ C and C ₆ rings	6.8(10)	8.0(4)
Angle between the N ₃ C ₂ and C ₆ rings	-	10.9(4)
Angle between the N ₃ C ₂ and benzyl rings	-	75.7(2)

Table S2. Crystal data and collection details for **ReAlkyne** and complex **9**·CH₂Cl₂.

Complex/Formula	ReAlkyne /C ₂₄ H ₁₃ N ₆ O ₃ Re	Complex 25 /C ₃₂ H ₂₂ Cl ₂ N ₉ O ₃ Re
<i>F</i> _w	619.60	837.68
<i>T</i> , K	295(2)	293(2)
<i>λ</i> , Å	0.71073	0.71073
Crystal system	Orthorhombic	Triclinic
Space Group	<i>Pccn</i>	<i>P</i> $\bar{1}$

a , Å	21.26(5)	9.8486(7)
b , Å	22.33(5)	12.8734(10)
c , Å	10.05(2)	14.2272(11)
α , °	90	73.2150(10)
β , °	90	78.726(10)
γ , °	90	70.6500(10)
Cell Volume, Å ³	4772(19)	1619.4(2)
Z	8	2
D_c , g cm ⁻³	1.725	1.718
μ , mm ⁻¹	5.130	3.966
F(000)	2384	821
Crystal size, mm	0.14×0.12×0.11	0.16×0.13×0.12
θ limits, °	1.322–23.817	1.504–27.146
Index ranges	-24 ≤ h ≤ 24 -25 ≤ k ≤ 25 -11 ≤ l ≤ 11	-12 ≤ h ≤ 12 -16 ≤ k ≤ 16 -18 ≤ l ≤ 18
Reflections collected	37501	18280
Independent reflections	3667 [$R_{int} = 0.2262$]	7117 [$R_{int} = 0.0403$]
Completeness to θ max	100.0%	99.7%
Data / restraints / parameters	3667 / 162 / 307	7117 / 24 / 424
Goodness on fit on F ²	0.963	1.012
R_1 ($I > 2\sigma(I)$)	0.0680	0.0424
wR_2 (all data)	0.2084	0.0968
Largest diff. peak and hole, e Å ⁻³	1.740 / -0.891	2.036 / -0.541

^1H and ^{13}C NMR of carbohydrate-appended Re(I) complexes

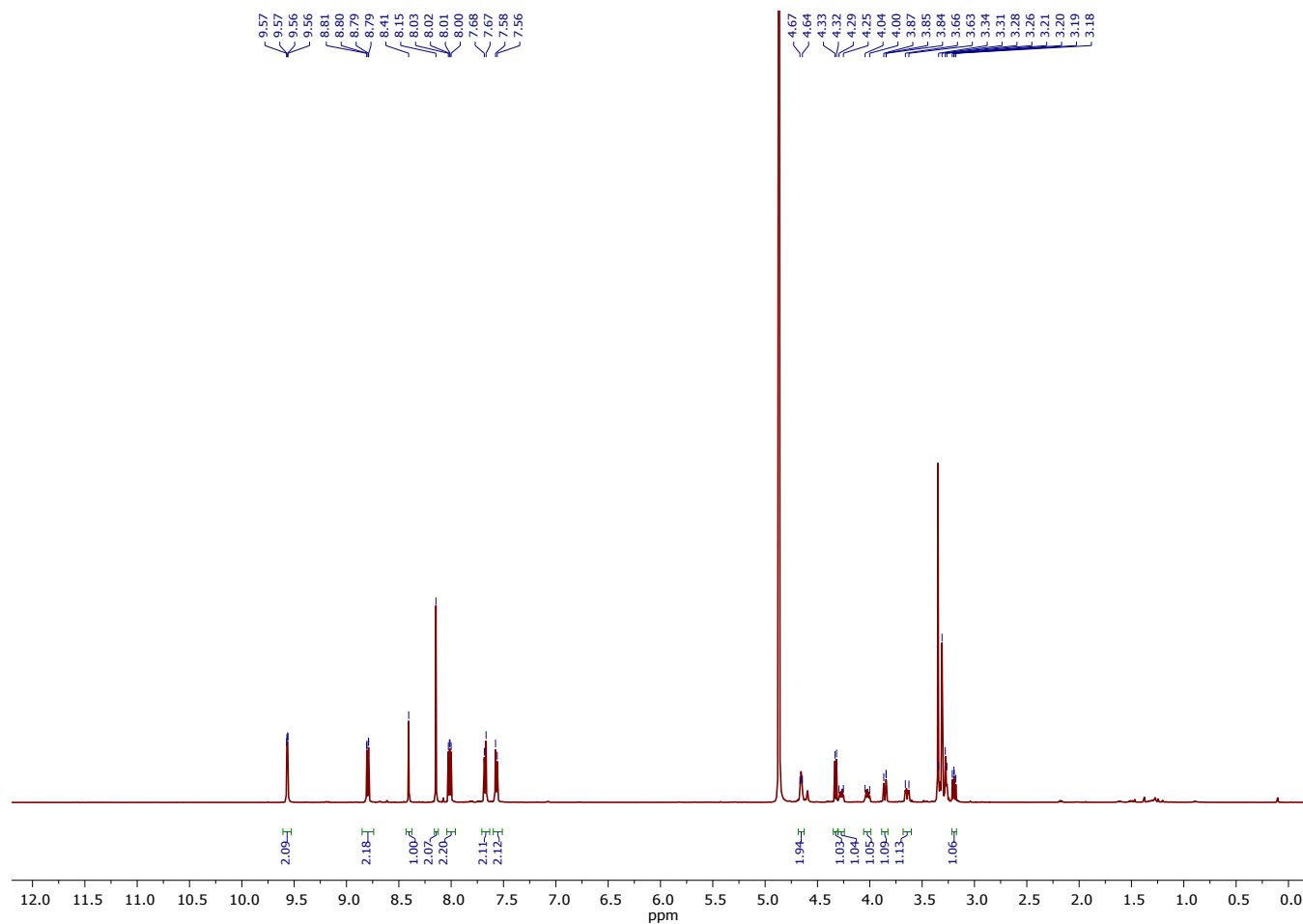


Figure S1. ^1H NMR (500 MHz) spectrum of **ReGlucose** in CD_3OD .

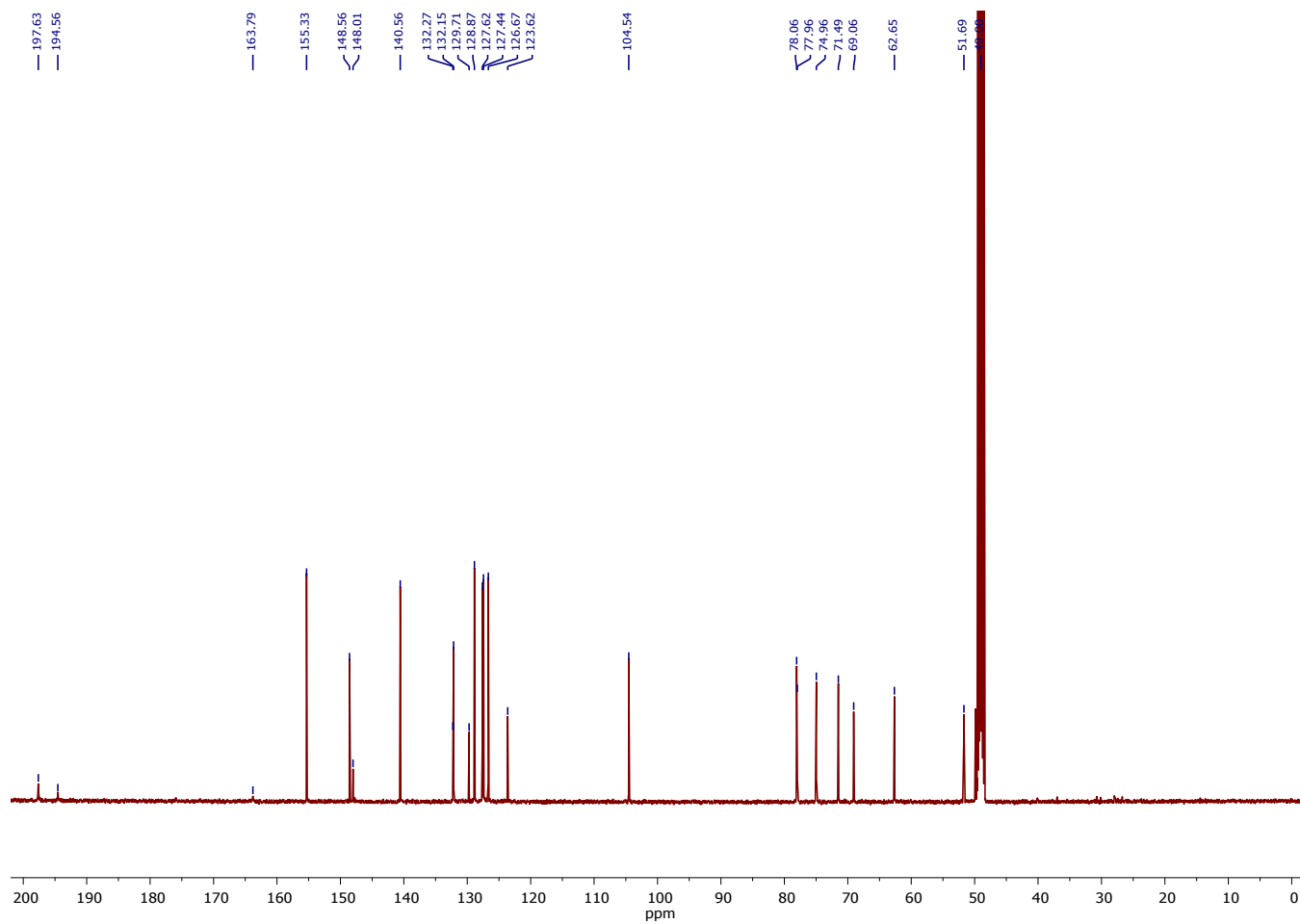


Figure S2. ^{13}C NMR spectrum of **ReGlucose** in CD_3OD .

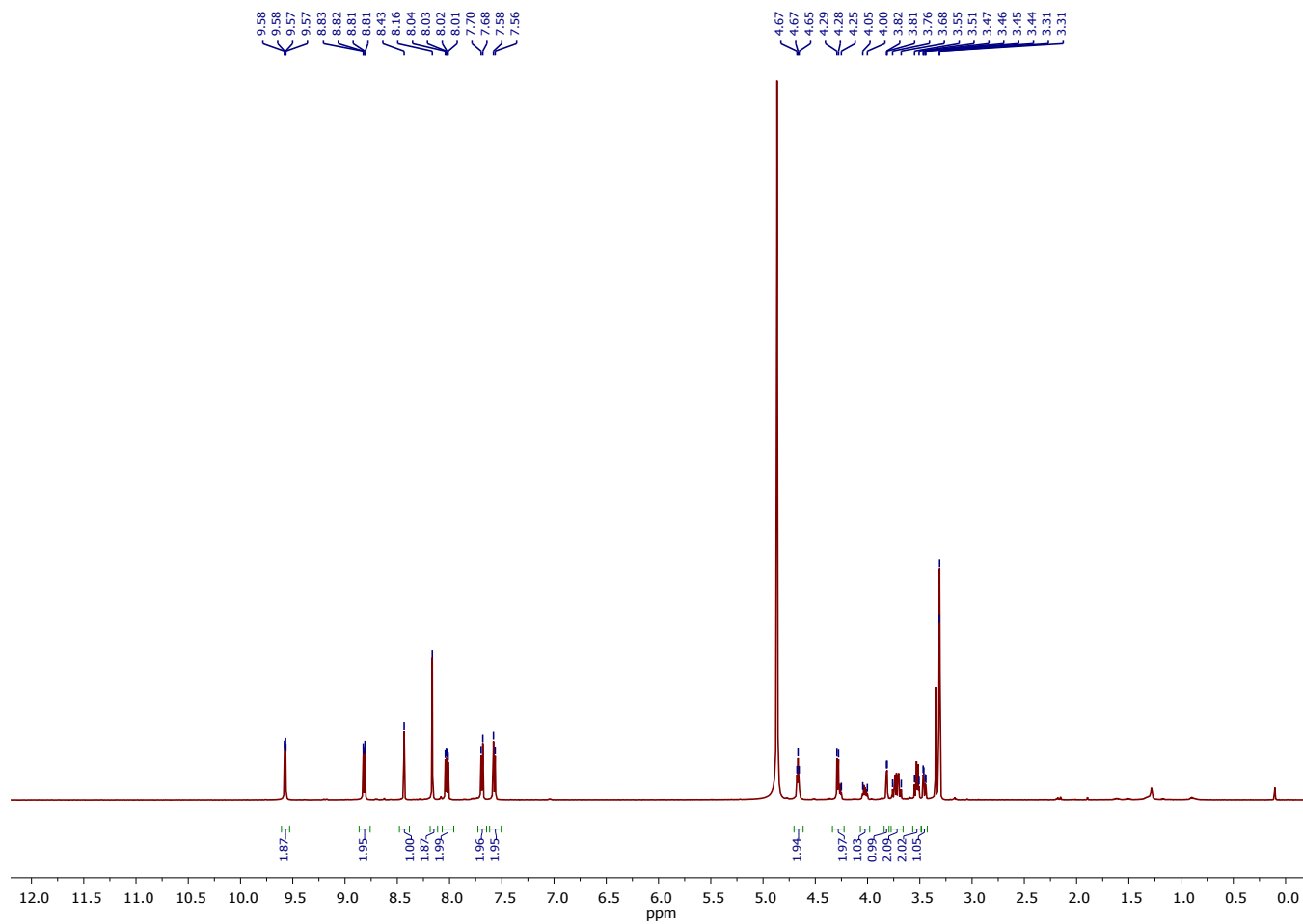


Figure S3. ^1H NMR (500 MHz) spectrum of ReGalactose in CD_3OD .

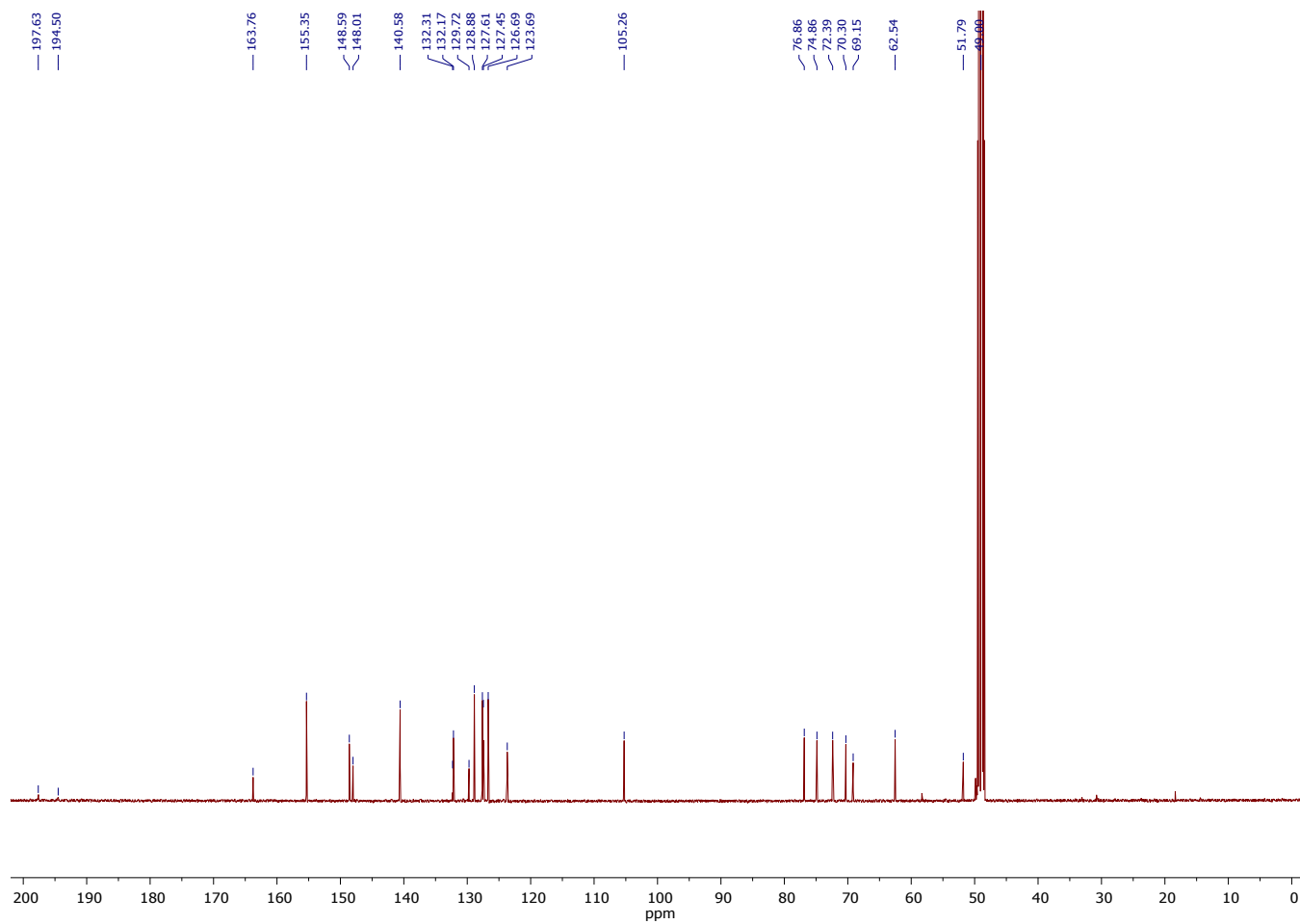


Figure S4. ^{13}C NMR spectrum of **ReGalactose** in CD_3OD .

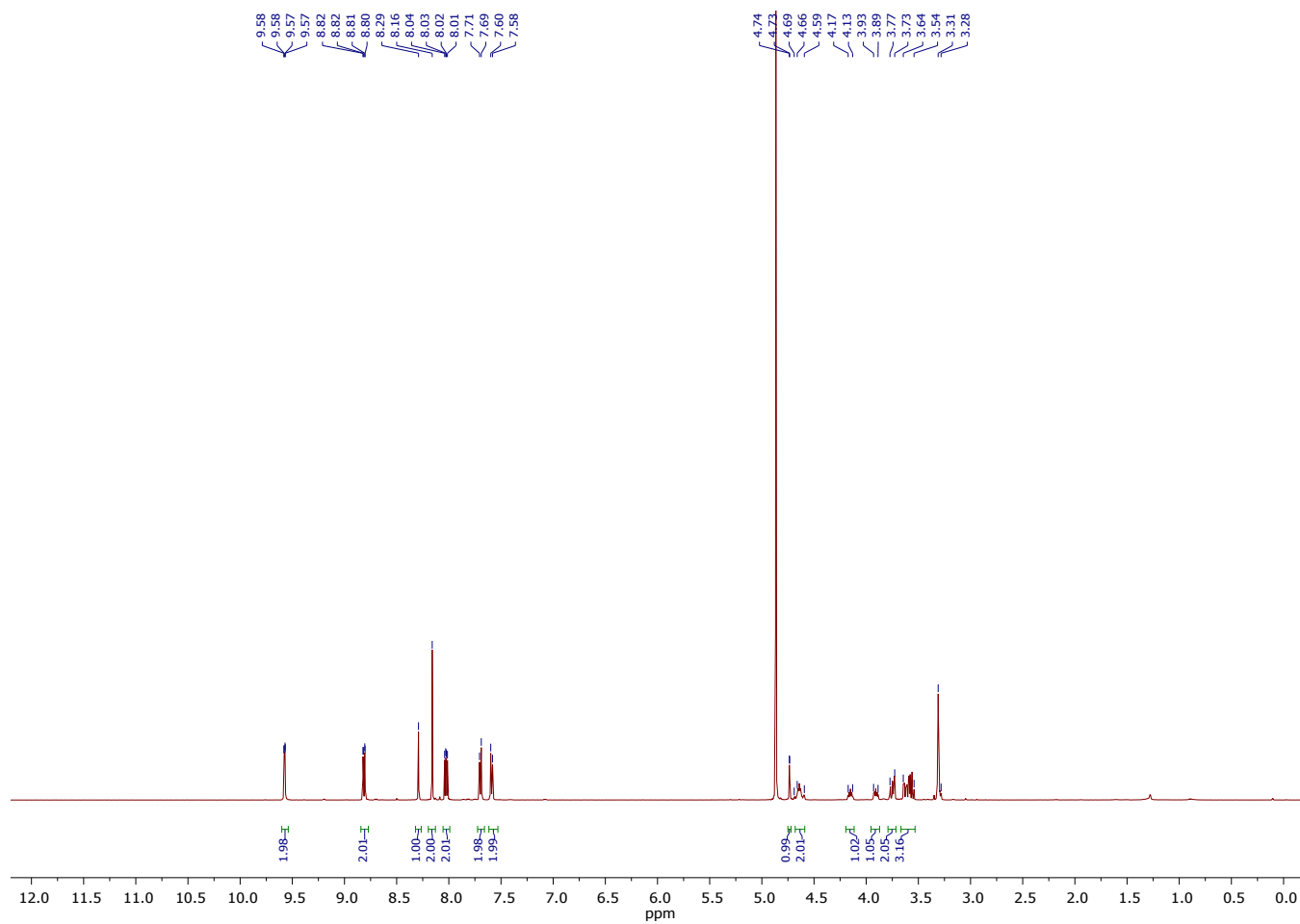


Figure S5. ¹H NMR (500 MHz) spectrum of **ReMannose** in CD₃OD.

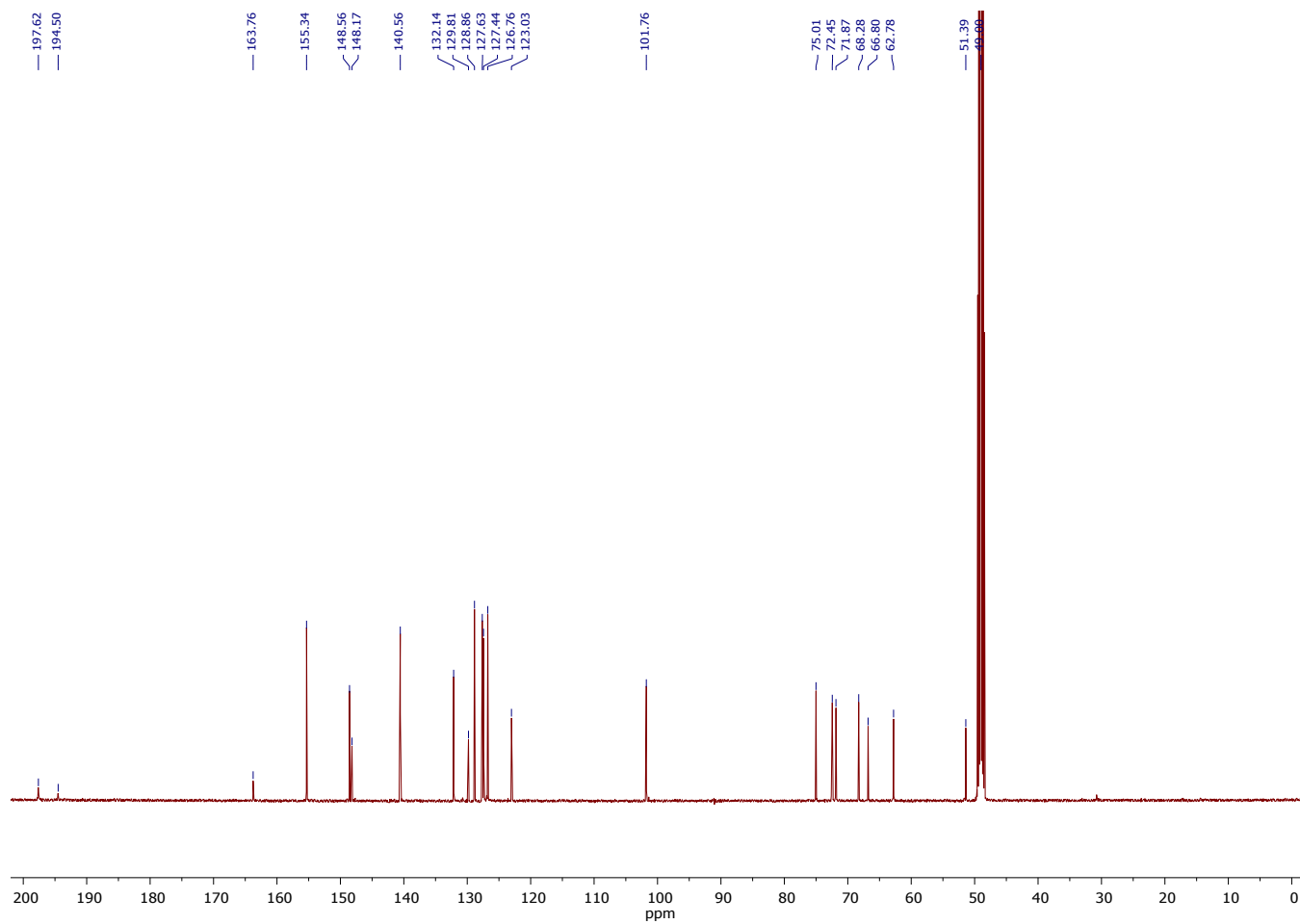


Figure S6. ^{13}C NMR (125 MHz) spectrum of **ReMannose** in CD_3OD .

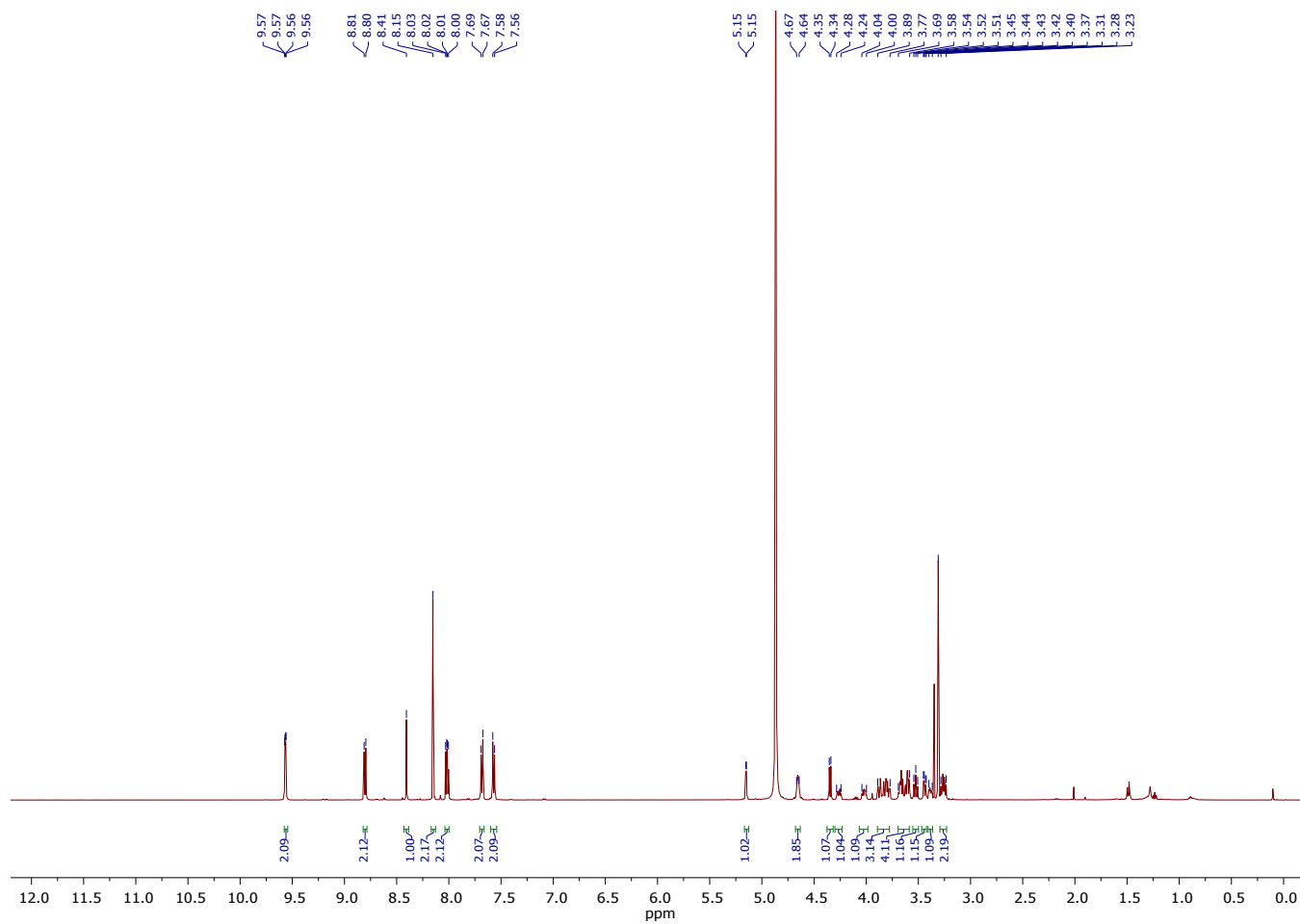


Figure S7. ^1H NMR (500 MHz) spectrum of **ReMaltose** in CD_3OD .

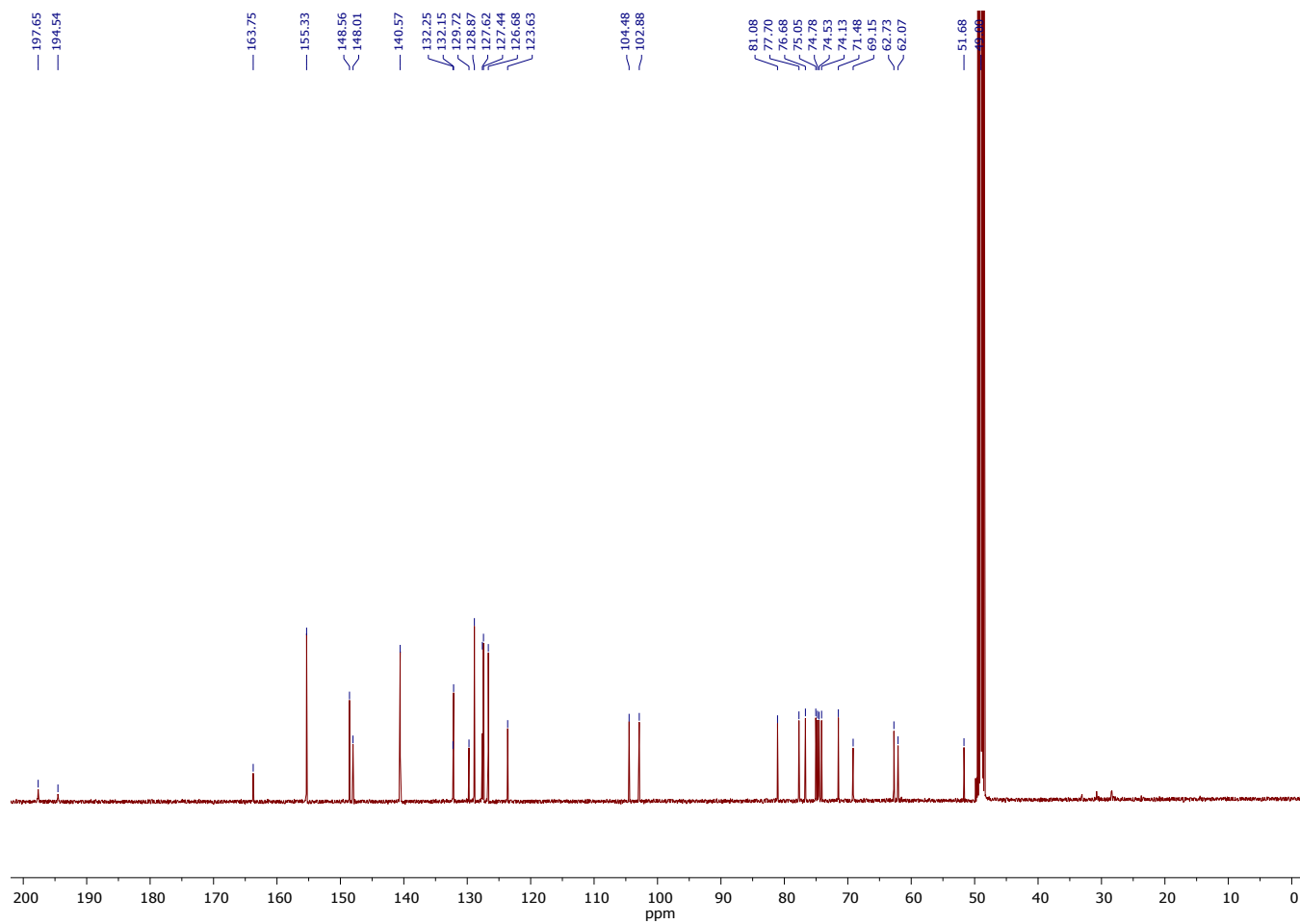


Figure S8. ¹³C NMR (125 MHz) spectrum of ReMaltose in CD₃OD.

HRMS spectra of carbohydrate-appended Re(I) complexes

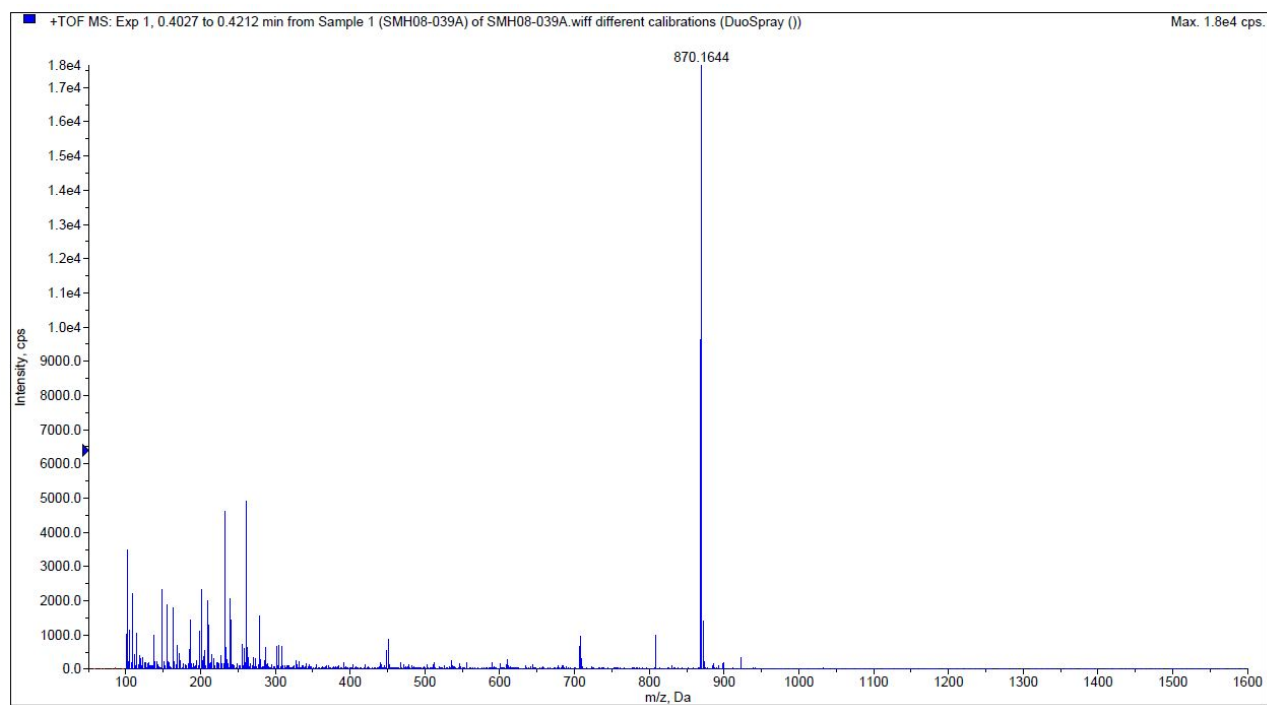


Figure S9. HRMS spectrum for ReGlucose.

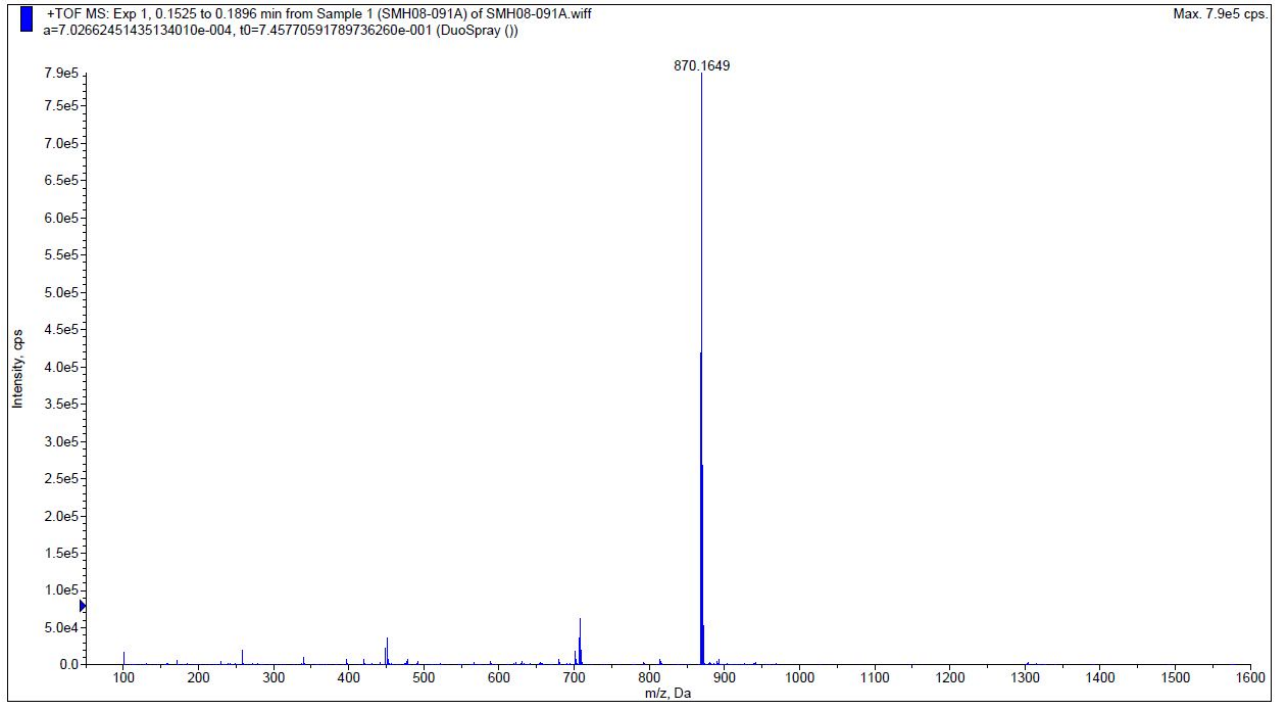


Figure S10. HRMS spectrum for **ReGalactose**.

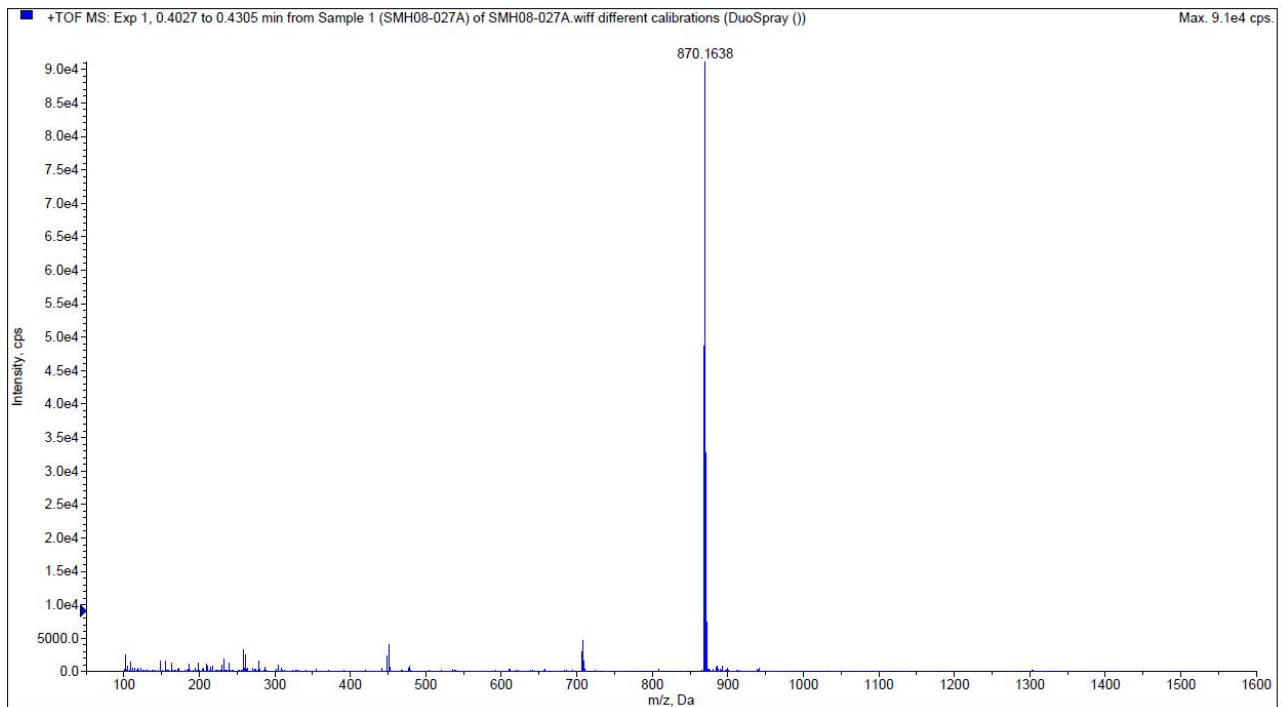


Figure S11. HRMS spectrum for **ReMannose**.

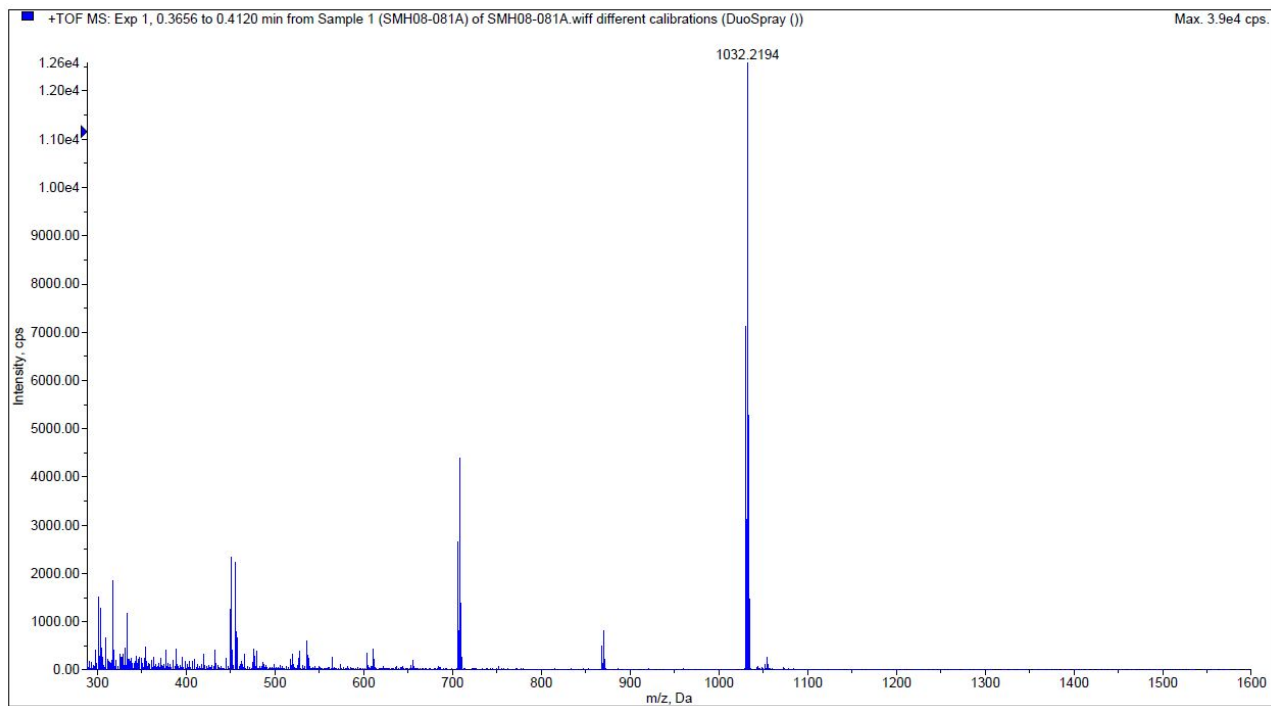


Figure S12. HRMS spectrum for **ReMaltose**.

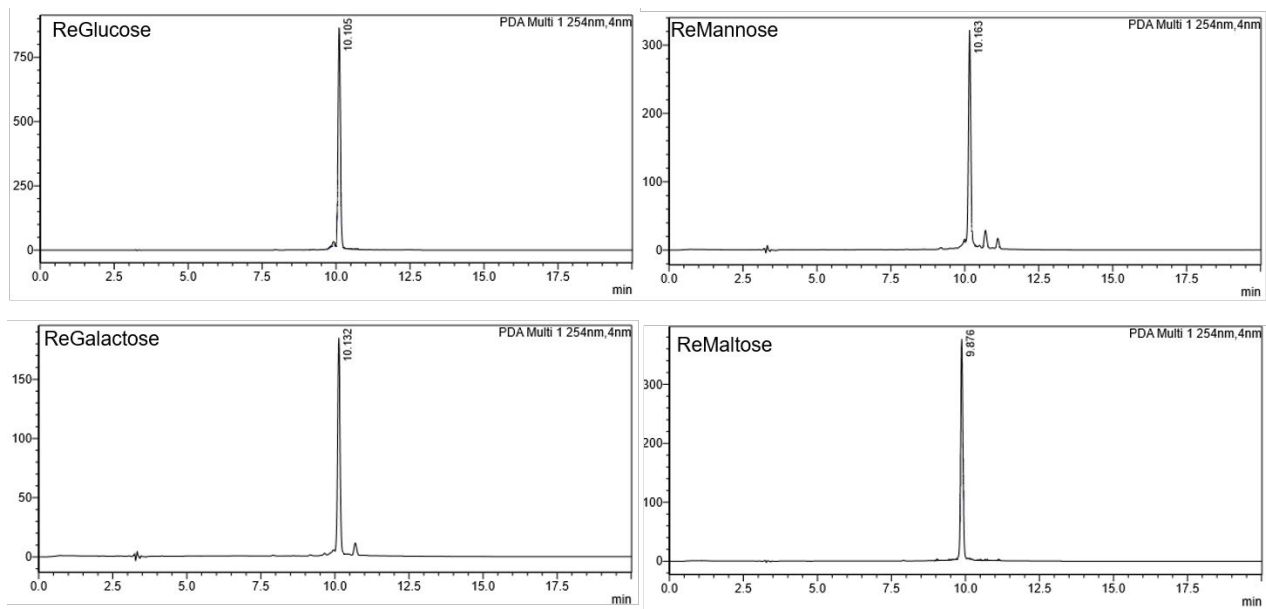


Figure S13. Analytical RP-HPLC of carbohydrate conjugated complexes; gradient 5% to 95% CH₃CN in H₂O containing 0.1% FA over 7 min at a flow rate of 1 mL/min, followed by 95% CH₃CN in H₂O containing 0.1% FA over 13 min.

Photophysics

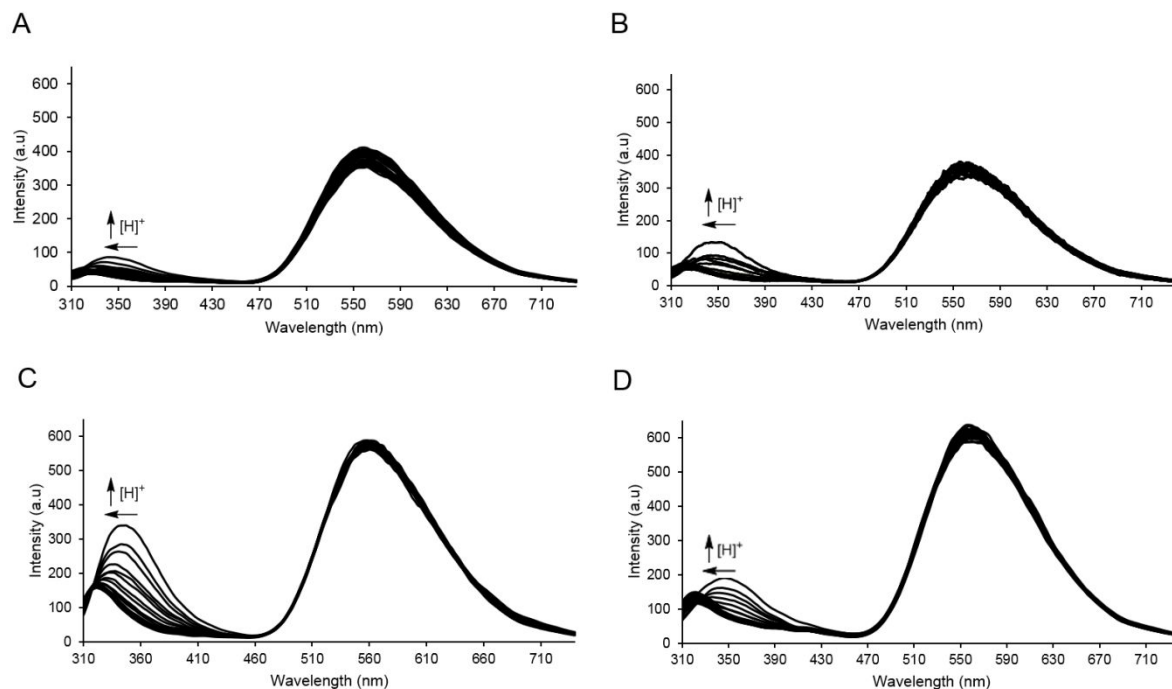


Figure S14. Emission profiles of sugar-appended Re(I) complexes at 275 nm excitation when titrated forward from pH 4–8 by addition of NaOH and in reverse by addition of HCl. Metal-centered emission remains stable, observable as a prominent emission band at 565 nm. An emission band at approximately 350 nm is observed to undergo a reversible hypsochromic shift to approximately 320 nm accompanied by a minute drop in intensity, this is attributed to a pH responsive shift in triazole emission and is observable in all four complexes. (A) **ReGlucose** 5×10^{-6} M, (B) **ReGalactose** 5×10^{-6} M, (C) **ReMannose** 5×10^{-6} M, (D) **ReMannose** 5×10^{-6} M.

10^{-5} M and (D) **ReMaltose** 5×10^{-5} M; Spectra recorded in 1:1 MeOH/H₂O with a constant ionic strength (I) of 1×10^{-3} M using NaCl.

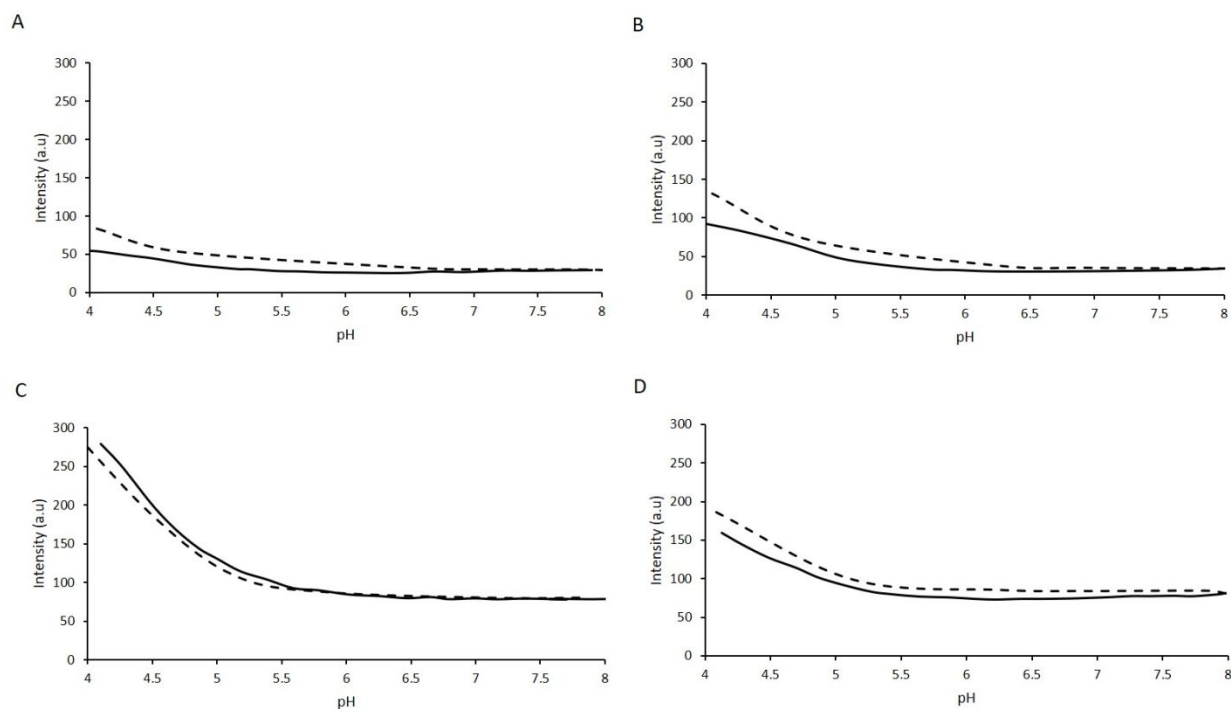


Figure S15. The change in emission intensity of the 350 nm triazole emission of each of the carbohydrate-appended rhenium ion complexes as a function of pH; (A) **ReGlucose** 5×10^{-6} M, (B) **ReGalactose** 5×10^{-6} M, (C) **ReMannose** 5×10^{-5} M and (D) **ReMaltose** 5×10^{-5} M; Spectra recorded in 1:1 MeOH/H₂O with a constant ionic strength (I) of 1×10^{-3} M using NaCl) at 275 nm excitation; forward (solid line) and back (dotted line) titration.

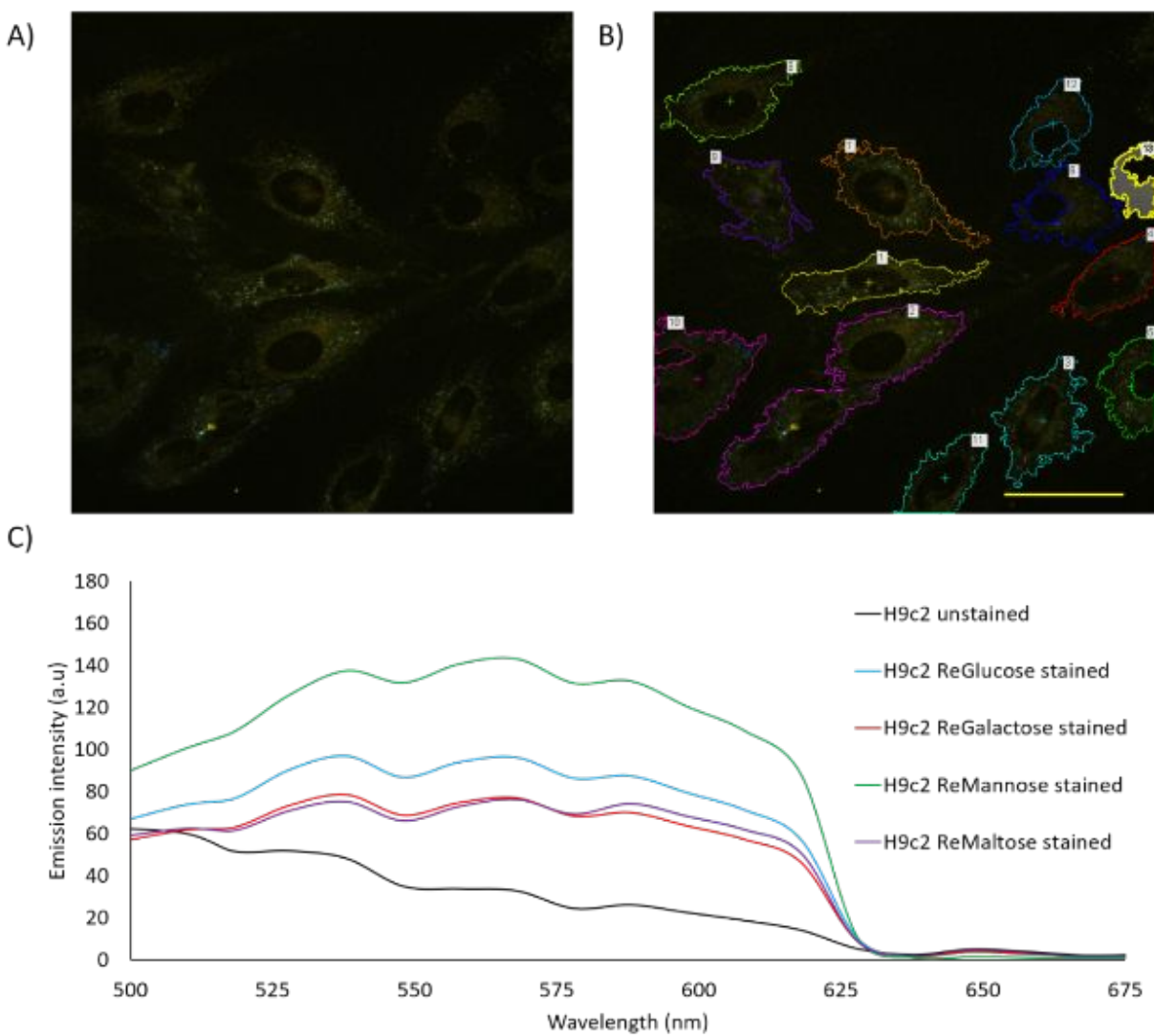


Figure S16. (A) Spectral image of H9c2 cells stained with **ReGlucose**. (B) Regions of interest in H9c2 cells for **ReGlucose** used to produce average for spectral plot. (C) Comparative spectral profiles of H9c2 cells that were unstained and stained with each carbohydrate-appended Re(I) complex. Scale bars: 50 μm .

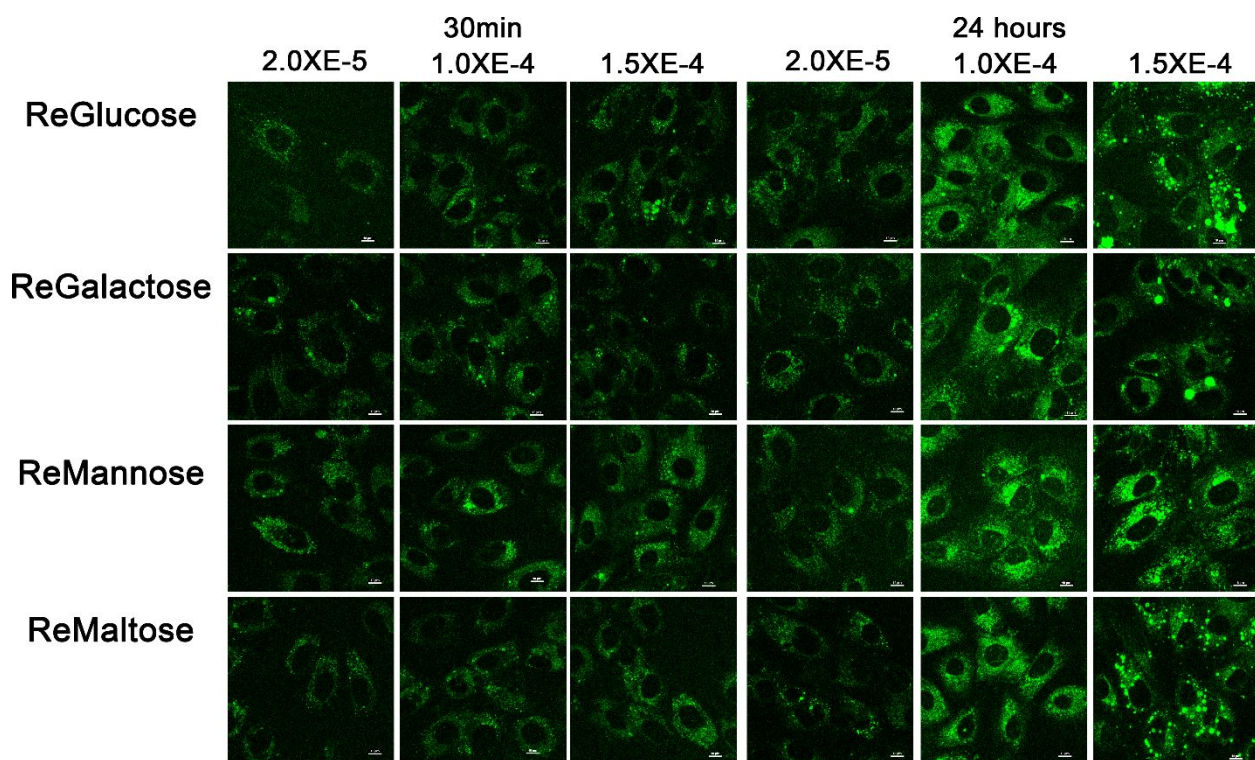


Figure S17. Micrographs showing concentration and time dependent accumulation of carbohydrate-conjugated Re(I) complexes in H9c2 cells. Scale bars: 10 μ m.

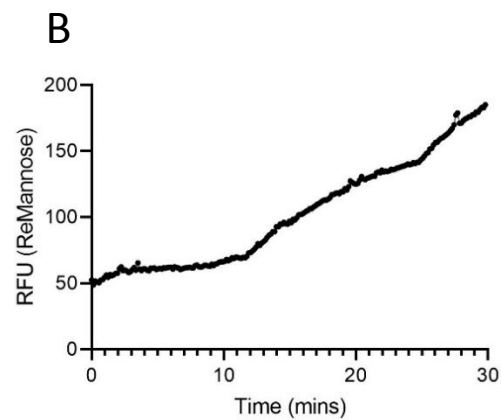
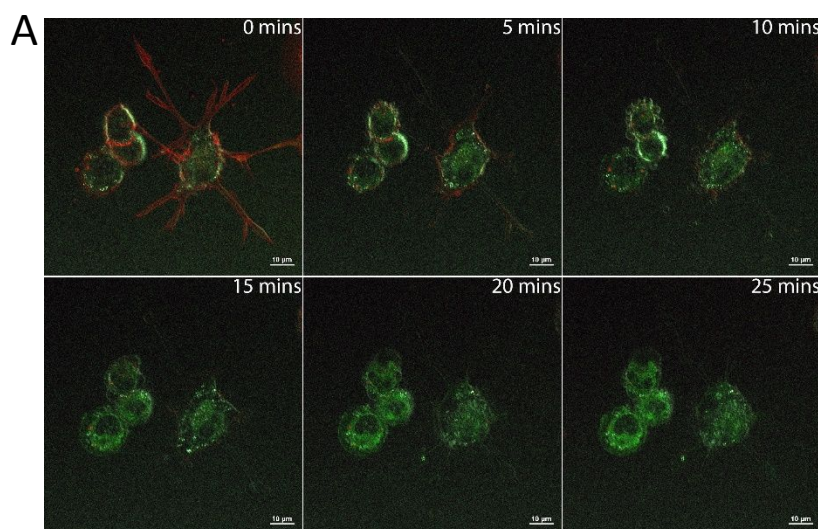


Figure S18. A) Micrographs showing cells over a 25 minute time-course experiment, Imaging of ReMannose at time 0 was done 20 seconds after adding the probe to the cell culture media. All micrographs were captured with no delay (~1 image per 8 seconds) for 25 minutes. with no change in the emission from **ReMannose**. B) Graph showing change in intensity of emission of ReMannose in micrographs, supporting photostability, mean intensity values from 4 THP-1 macrophages were obtained and plotted using GraphPad Prism software (n=4; mean \pm SEM).

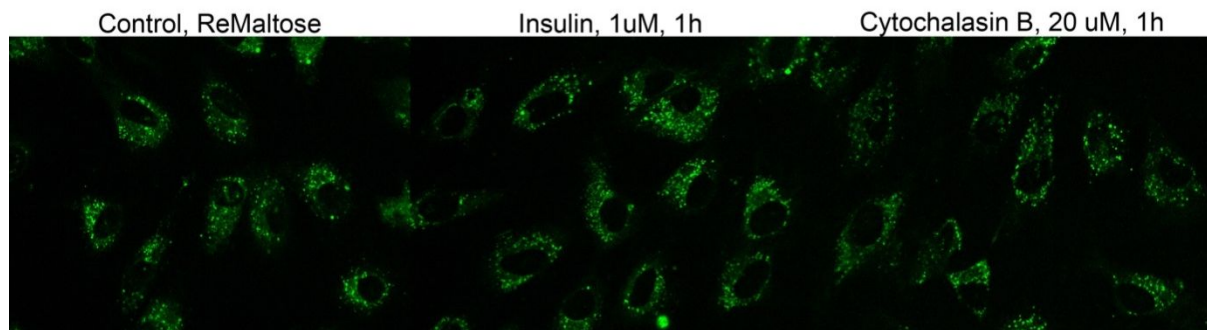


Figure S19. Uptake of **ReMannose** by H9c2 cells. Scale bars: 50 μ m.

Table S3. Pearson co-efficient for co-localisation between organelle markers

LysoTracker™ and ER Tracker™ and Re(I) complexes in H9c2 cells.

	<i>ReGlucose</i> (Mean ± StDev)	<i>ReGalactose</i> (Mean ± StDev)	<i>ReMannose</i> (Mean ± StDev)	<i>ReMaltose</i> (Mean ± StDev)
<i>LysoTracker™</i>	0.423 ± 0.085	0.564 ± 0.117	0.561 ± 0.139	0.508 ± 0.041
<i>ER Tracker™</i>	0.235 ± 0.088	0.547 ± 0.140	0.509 ± 0.061	0.621 ± 0.029

Cell viability

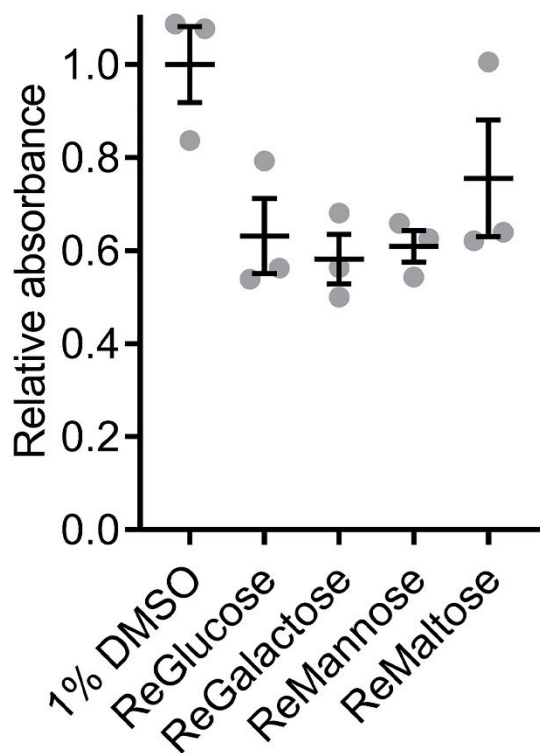


Figure S20. Viability of H9c2 cells following a 24 h incubation with the carbohydrate-conjugated Re(I) complexes. The results are reported as the mean absorbance, relative to a vehicle control (n = 3; mean ± SEM).